Elastic constants and Debye temperature of bcc ^{3}He

D. S. Greywall
Bell Laboratories, Murray Hill, New Jersey 07974
(Received 17 September 1974)

Measurements of the longitudinal, the fast-transverse, and the slow-transverse sound velocities have been made in single crystals of bcc ^{3}He at 24.45 cm^3/mole and at 0.4 K. The quality and orientation of the crystals were determined using x rays. The reduced elastic constants, in units of 10^9 cm^2/sec^2, $C_{11}/\rho = 1.634 \pm 0.020$, $C_{12}/\rho = 1.356 \pm 0.033$, and $C_{44}/\rho = 0.753 \pm 0.010$ resulted from a least-squares fitting of the data. These constants yield a compressibility which is in agreement with the results of thermodynamic measurements and a Debye temperature which is consistent with $\Theta_D^{\max}$, the maximum value of the temperature-dependent calorimetric Debye temperature. Existing sound-velocity data at 21.66 cm^3/mole were reanalyzed with the results, in units of 10^9 cm^2/sec^2: $C_{11}/\rho = 2.727 \pm 0.033$, $C_{12}/\rho = 2.477 \pm 0.058$, and $C_{44}/\rho = 1.422 \pm 0.021$. These constants also yield a compressibility in agreement with thermodynamic measurements. Only C_{12} is significantly different (4%) from the constants previously reported. As an important consequence, however, $(C_{11} - C_{12})/2\rho$, the modulus corresponding to the slow-transverse velocity in the $\langle 110 \rangle$ direction, is considerably larger. The Debye temperature calculated using these constants is not inconsistent with $\Theta_D^{\max}$. This result is contrary to that previously reported. At neither density is there evidence to suggest that any of the anomalous specific heat must be due to an anomalous phonon dispersion.

I. INTRODUCTION

The low-temperature specific heat C_v of bcc ^{3}He has been the subject of considerable interest during the past several years.[1] Even at the lowest temperatures, what is expected to be only the lattice specific heat does not have the usual Debye T^3 dependence; there is an excess specific heat.[2-6] The comparison to the limiting Debye behavior is usually made by defining a temperature-dependent Debye temperature $\Theta_D^c(T)$ through the relation

$$C_v = \tfrac{12}{5}\pi^4 R[T/\Theta_D^c(T)]^3. \quad (1)$$

Departures from T^3 behavior are then seen in a plot of $\Theta_D^c(T)$ as deviations from a constant value. For most solids,[7] including hcp ^{4}He,[3,6,8-10] $\Theta_D^c(T) \approx \Theta_D^c(0\ \mathrm{K}) \equiv \Theta_D$ for $T/\Theta_D \lesssim 0.02$. For bcc ^{3}He, $\Theta_D^c(T)$ has a maximum $\Theta_D^{\max}$ near $T/\Theta_D^{\max} \approx 0.02$ and decreases rapidly with decreasing temperature.

Several suggestions as to the possible source of this anomaly have been put forth.[1] At one time a most promising conjecture attributed the observed phenomena to an anomalous upward-curving phonon dispersion implying an extremely large elastic anisotropy. An upward curvature of the phonon spectrum in some directions, confined to low energies, would lead to an apparent excess specific heat at low temperatures.[11] The ordinary T^3 dependence of C_v would in this case be seen only at extremely low temperatures. The requirement of a large elastic anisotropy was necessary to explain the fact that the then existing measurements of the transverse sound velocity[12] in ^{3}He samples, which may have been polycrystalline, suggested a Θ_D even larger than $\Theta_D^{\max}$. Taken as the principal evidence that the phonons were probably the modes contributing the excess specific heat were measurements of the thermal conductivity.[5] If the phonons are the only modes responsible for the transport of heat energy, then at low temperatures the thermal conductivity is proportional to the *lattice* specific heat. The measured thermal conductivity was found to be proportional to an extrapolation of the *measured* anomalous specific heat. The conclusion drawn was that the excitations responsible for the excess specific heat must transport heat energy in essentially the same way as the phonons in the system.

Measurements of the sound velocity in single crystals of bcc ^{3}He of known orientation followed.[13] These data yielded a Θ_D which was less than $\Theta_D^{\max}$ and supported the idea of an anomalous phonon dispersion. If the phonons were not at all responsible for the anomalous specific heat, then the real Θ_D corresponding to the lattice specific heat alone, as determined from the sound-velocity measurements, would be greater than or equal to $\Theta_D^{\max}$, depending on the temperature dependence of the excess contribution to C_v. It thus seemed apparent that measurements of the specific heat at even lower temperatures would show that with decreasing temperature, $\Theta_D(T)$ was leveling off to a constant value. This, however, turned out not to be the case.

The most recent measurements of C_v,[6] which extend down to below 65 mK ($T/\Theta_D^{\max} \approx 0.004$), can be described well, after a nuclear spin-ordering contribution has been subtracted off, by a function which contains in addition to a term proportional

to T^3, a term linear in T. The corresponding $\Theta_D^c(T)$ falls below the Θ_D determined by the sound-velocity measurements and appears to be heading towards 0 K. In addition, the low-temperature specific heat is not proportional to the measured thermal conductivity.[5]

It becomes difficult then to retain the notion that all of the anomaly is due to the phonons themselves. The possibility of a strongly temperature-dependent phonon spectrum has been experimentally tested through precise measurements of the temperature dependence of the sound velocities down to 123 mK.[14] There remained the chance that the specific heat measured at low-temperatures sampled long-wavelength phonons with a much smaller average velocity than the appropriate average of the sound velocities measured at higher temperatures. The Debye temperature determined from elastic measurements, $\Theta_D^e(T)$, could thus have a large temperature dependence and only be equal to Θ_D in the limit $T \to 0$ K. As expected,[15] however, these measurements showed the $\Theta_D^e(T)$ is only a weak function of the temperature and that to a good approximation, at least for the larger molar volumes, $\Theta_D^e(T) \approx \Theta_D$.

The experimental evidence thus appears to indicate that perhaps some but certainly not all of the excess specific heat may be due to an anomalous phonon dispersion. An estimate of how much of the excess must be attributed to the phonons can be inferred using the Θ_D determined by sound-velocity data in crystals of known orientation. Such measurements, as mentioned above, exist.[13] However, some question[16] has been raised concerning the orientation of a few of these crystals and no direct measurements of a slow-transverse velocity were made in this study to confirm the accuracy of the slow-transverse velocity surface implied by the measurements of the longitudinal and fast-transverse velocities. The elastic Θ_D is most strongly influenced by the slow-transverse velocity surface. Other measurements[14] of the sound velocity in crystals of unknown quality and orientation yield only an upper limit to Θ_D which is less than $\Theta_D^{\max}$.

In this paper we report new measurements of the sound velocity in x-ray-oriented single crystals of bcc ^{3}He at a molar volume of 24.45 cm^3. This molar volume was chosen to be near that at which the temperature dependence of the sound velocities is known. These data include measurements on the slow-transverse velocity surface and indicate $\Theta_D = 18.53 \pm 0.66$ K in excellent agreement with $\Theta_D^{\max}$. This suggest that perhaps *none* of the excess specific heat is due to the phonons.

The details of the experimental techniques are given in Sec. II. In Sec. III the results of the sound-velocity measurements are presented. Also given are the complete set of elastic constants which best describe the velocity data, and the compressibility and Θ_D determined by these constants. Comparisons are made with measurements by others. The results of a reanalysis of previously published sound-velocity data[13] obtained in crystals of known orientation at a higher density are included. A summary is provided in Sec. IV.

II. EXPERIMENT

A. Freezing cell

The freezing cell used in this work is in many respects quite similar to one described in an earlier publication.[13] There were, however, several modifications incorporated into the present design. A cross-sectional drawing is shown in Fig. 1. The total cell volume was 0.43 cm^3; the volume between the ultrasonic transducers was 0.32 cm^3.

The sealing of the plexiglass cell body, with its large thermal contraction, to the copper end caps of the cell was accomplished by first epoxying[17] a copper shoe to each end of the cell body and then using the usual indium O-ring seal. The plastic-to-copper epoxy seals were made by potting the thin circular fins (0.025 cm thick, 0.15 cm high), machined as part of the copper shoes, into narrow annular grooves (0.04 cm wide) cut into the ends of the cell body. The indium O rings were compressed by pulling the cell body against each end cap with four 6-32 stainless-steel screws. The screws, maximum torque of 50 in. oz, passed

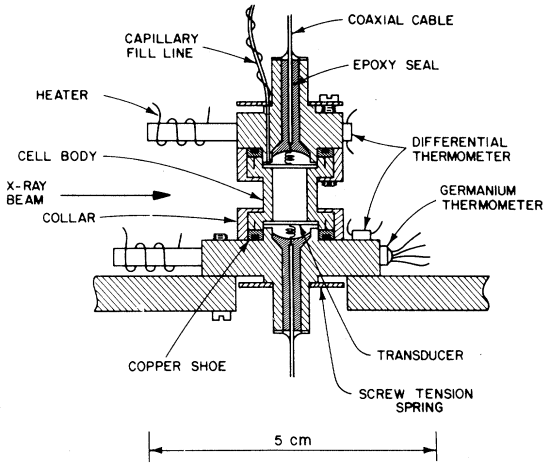

FIG. 1. Freezing cell.

through the end caps and threaded into stainless-steel collars which slipped over the flanges machined as part of the cell body. Screw tension was maintained during cooling by 0.15-cm-thick phosphor-bronze springs.

The quartz ultrasonic transducers were held against shoulders cut in the cell body with 0.013-cm-thick phosphor-bronze wave springs (not shown in the figure). These springs also made the electrical ground contact to the coaxial gold plating on the transducers. The active electrical contact to each of the transducers was made with the 0.013-cm-diam coiled center conductor of a miniature coaxial cable. Each cable was sealed into the end caps with epoxy.[18]

The helium sample entered the cell through a stainless-steel capillary passing through the top end cap. The capillary was wrapped with a 10-kΩ heater. The volumes in the cell separated by the transducers were joined by shallow grooves milled into the shoulders of the cell body. The main thermometer was a Cryocal[19] germanium resistor (CR100) mounted on the bottom end cap. In addition, a differential thermometer consisting of a pair of carbon resistors was mounted on the top and bottom end caps of the cell. Each resistor actually consisted of a bank of six 56-Ω Allen-Bradley carbon resistors connected in series. The resistors were first ground flat on one side to improve the thermal contact and then attached to the cell end caps with GE7031 varnish. A thin sheet of Mylar provided the electrical insulation. 10-kΩ Karma-wire[20] heaters were wound onto $\frac{1}{8}$-in copper rods which had been soldered into each of the end caps.

B. Cryostat

A drawing of the lower portion of the cryostat is shown in Fig. 2. For clarity the various components on each of the platforms have been drawn as if they were located in a single plane. These components were drawn approximately to scale. A 10-cm scale length is indicated at the bottom of the figure.

Each of the four platforms was machined from oxygen-free high-conductivity copper. The uppermost (4 K) platform was the bottom of a 12-l helium reservoir. The copper plate was joined to the stainless-steel flange of the Dewar using an intermediary length of thin-walled stainless-steel tubing. The tubing was hard soldered to the copper plate and helium arc welded to a stainless-steel flange which was then sealed against the Dewar flange with an indium O ring. Located below the 4-K platform was the 1-K cold plate. This platform was cooled to a temperature of 1.2 K with a continuous ^{4}He refrigerator.[21] Liquid ^{4}He from the main bath entered the evaporator chamber by first flowing through a sintered copper filter and then through a flow impedance. The flow impedance consisted of a 72-cm length of 0.020-cm-i.d. stainless-steel tubing into which a 0.018-cm stainless-steel wire had been inserted. ^{3}He gas which had been precooled to 4 K was condensed at this platform. The liquid ^{3}He, after flowing through an impedance identical to the one on the ^{4}He refrigerator, entered the ^{3}He evaporator of a continuous ^{3}He refrigerator. This platform was normally operated at a temperature of about 0.35 K. The sample platform was firmly positioned below the 0.3-K platform with four 0.32-cm-diam stainless-steel rods approximately 13 cm long. These rods also provided a thermal connection between the two platforms with a conduction of 2.4×10^{-5} W/K at 1 K. The conduction could be increased by an order of magnitude by closing the mechanical heat switch. The freezing cell was attached to this platform with four No. 4-40 stainless-steel screws. The thermal contact between the bottom copper end cap of the cell and the copper platform was improved with a coating of Apiezon *N* grease. The helium sample entered the cell through a stainless-steel capillary. After a length of 18 cm, the capillary entered its own vacuum system and passed out of the Dewar. Between the cell and the bottom of the thin-walled stainless-steel vacuum tube the capillary had dimensions 0.02-cm i.d., 0.04-cm o.d. From this point out to the gas-handling system the capillary had dimensions 0.05-cm i.d., 0.08-cm o.d. At the union the capillary was thermally connected to the 1-K platform with a copper wire which provided about 10^{-3} W/K conduction at 1 K. A heater mounted on the union could be used to keep the temperature at this point above the

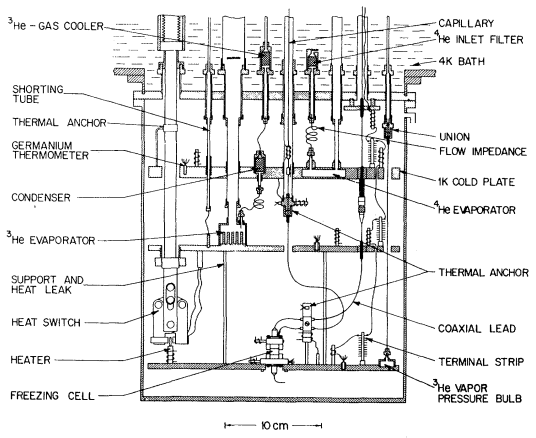

FIG. 2. Cryostat.

freezing temperature of the helium sample. To keep the heat leak into the top of the freezing cell to a minimum, thereby reducing temperature gradients in the solid sample, the capillary was also thermally anchored to the sample platform at a point approximately 7 cm from the cell. The thermal contact was made by mechanically clamping the copper sleeve hard soldered to the capillary against a copper block which was in turn thermally connected (10^{-3} W/K) to the sample platform. A heater wound on the anchor block permitted the temperature to be raised above the freezing temperature during the growth of a solid helium sample.

The electrical leads coming from room temperature down to the 4-K platform were Formvar-insulated 0.013-cm manganin wires. Below this level the leads were Formvar-insulated 0.0076-cm manganin wires. At each level the leads were thermally anchored by wrapping the wires around 0.32-cm-diam copper posts soldered to the platforms and then encapsulating the wire-covered posts with GE 7031 varnish. The various heaters were made in a similar manner using 0.0038-cm Karma wire. All heaters had a nominal resistance of 10 kΩ. Four miniature coaxial cables[22] were brought from room temperature to the 1-K platform. They were electrically insulated from, but thermally anchored to, the 4- and 1-K platforms with high-thermal-conductivity epoxy.[18] The cables had a 0.013-cm-diam silver-plated copper-clad steel center conductor and a 0.050-cm-o.d. stainless-steel outer conductor. The two coaxial cables continuing on to the cell had niobium center conductors and lead coated stainless-steel outer conductors.

C. X-ray system

A cross-sectional drawing of the cryostat at the level of the midpoint of the freezing cell is shown in Fig. 3. Both the 4- and 77-K thermal radiation shields were fabricated from heavy walled square aluminum tubing and were highly polished. All of the vacuum spaces were joined. This feature prevented the use of a transfer gas in the innermost chamber during the cool down of the apparatus, but it did eliminate the need for vacuum-tight seals on the 4-K x-ray windows. The windows on the 4- and 77-K shields were 0.00076-cm-thick aluminum foil. Aluminized Mylar was initially tried but the thermal shielding provided was not adequate; the sample platform could not be cooled below 0.54 K. The smaller room-temperature window was 0.038-cm-thick beryllium-foil; the exit window was 0.015-cm-thick Mylar. An attempt was made to use a 0.05-cm-thick beryllium foil for the room-temperature exit window but the material tested was not sufficiently fine grained. The set of exit windows had a total open angle of 80°.

The x-ray tube shield which contained a tungsten tube was mounted on a table which had vertical as well as horizontal degrees of freedom. A Polaroid x-ray camera was also mounted on this table. With the system at room temperature and the tail sections of the Dewar removed, the camera mounting platform was adjusted to be accurately parallel with the bottom of the cell. The film plane was then set at 5 cm from the midpoint of the cell. Using a fluorescent screen the x-ray tube was roughly positioned so that the beam struck the cell near its center. When the system was cold the position of the x-ray beam relative to the freezing cell was accurately determined using long-exposure-time photographs; the background in the photographs, caused by the x-rays scattered by the plastic cell body, clearly showed the shadows cast by the stainless-steel collars (see Fig. 1) of the freezing cell. For most of the helium crystals, transmission Laue photographs were taken only with the x-ray beam centered in the cell. In the few crystals for which a series of photographs were taken over the whole region in which the sample could be probed, no change in orientation and only small changes in quality were detected. All photographs were taken at a tube potential 50–55 kV and at a current 25–30 mA. With the particular collimator used, the exposure time was 10 min using type 57 Polaroid film. In the bcc ^{3}He samples only (110)- and (200)-type reflections were observed. With the large difference in intensity for these two reflections, all bright spots could be immediately classified at 110. The total uncertainty in both θ and φ is estimated to be about ±1°.

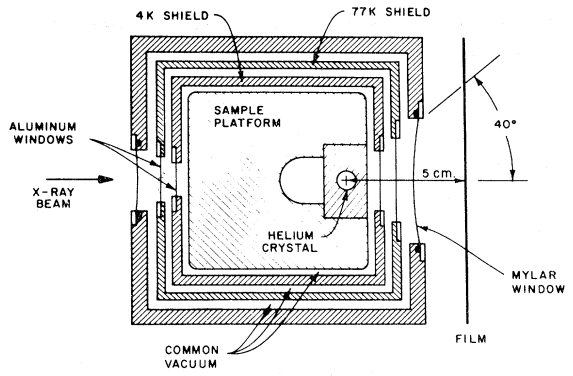

FIG. 3. Cross-sectional drawing of the cryostat at the level of the midpoint of the freezing cell.

D. Thermometry

The resistance of the germanium thermometer[19] located on the sample platform was measured using a dc technique. The thermometer was calibrated against the vapor pressure of ^{3}He in the range 0.5–2.4 K using the 1962 ^{3}He vapor-pressure scale.[23] The vapor pressure was measured using a Texas Instruments precision pressure gauge containing a 0–300-Torr quartz bourdon tube. Thermomolecular pressure corrections were applied.[24] The vapor-pressure line leading from the 4-K platform up to room temperature had an internal diameter of 0.27 cm which necessitated a pressure correction at 0.5 K corresponding to a temperature correction of 4 mK. The thermometer calibration was extended down to 0.27 K using the magnetic susceptibility of cerium-magnesium nitrate. The resistance-temperature data in the range 0.27–1.4 K were fitted to the expression

$$\ln R = A \ln T + B T^{-1/3} + C .$$

Systematic deviations from this function were less than 2 mK.

Near the melting curve the temperature was monitored using a sensitive ac-bridge technique.[25] The temperature-dependent element of the circuit was a germanium thermometer; the reference was a 1-kΩ Karma-wire-wound resistor. Both the thermometer and the reference were mounted on the bottom end cap of the cell. The bridge ratio was calibrated against the germanium thermometer on the sample platform.

The temperature difference between the top and bottom of the cell was measured with a second ac bridge circuit which compared the resistances of nearly identical carbon thermometers mounted on the top and bottom end caps of the cell (see Fig. 1). The differential thermometer was calibrated near the melting temperature by first filling the cell with a solid helium sample and then raising the temperature of the bottom of the cell above the melting temperature T_m. The solid, at its melting temperature in the upper portion of the cell, was insulated from the warmer bottom end cap of the cell by the liquid ^{3}He layer and melted slowly. The recorded differential bridge ratio thus corresponded to a $\Delta T \equiv T_{\text{bottom}} - T_{\text{top}}$ of $T - T_m$.

E. ^{3}He sample

The ^{3}He gas sample purchased had a stated ^{4}He impurity level of 200 ppm. The gas was purified further by distillation[26] and had a final ^{4}He concentration determined by mass spectrometry[27] of less than 17 ppm. The sample was stored in one of the 8-l cylinders shown in Fig. 4 at near atmospheric pressure.

F. Sound-velocity measurements

The velocity of sound in the helium crystals was measured using a double-ended pulse-echo technique. Most of the velocity measurements, both longitudinal and shear, were made using 10-MHz AC-cut quartz transducers. A few longitudinal velocity measurements were made using 10-MHz X-cut quartz transducers.

The voltage burst applied to the drive transducer had an amplitude that was varied in the range 1–10 V peak to peak and a duration that was varied in the range 1–10 μsec. The transmitted and received signals, after amplification and rectification, were displayed on one trace of a dual-trace oscilloscope. Also displayed was a variable-width square pulse. The leading edge of the square pulse was adjusted to coincide with the leading edge of the transmitted pulse. The trailing edge of the square pulse was adjusted to coincide with the leading edge of one of the received pulses. The time interval between the transmitted and each of the received pulses was accurately determined by measuring the width of the square pulse with an electronic timer. The accuracy of these time-interval measurements was limited by the rise times of the ultrasonic signals. The time interval between pulses was then determined by simply calculating the difference between the appropriate

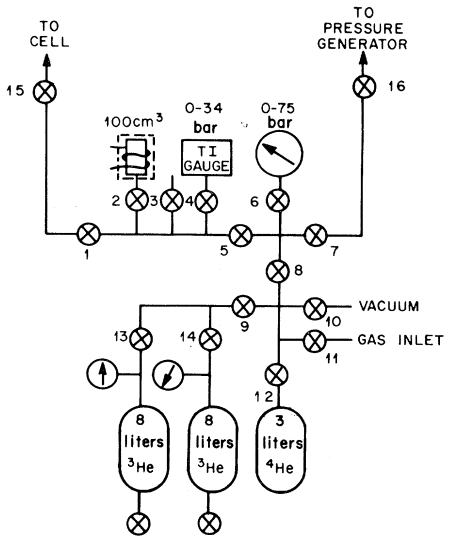

FIG. 4. Gas-handling system.

readings. Possible electronic delays were thus unimportant. The transit time for sound to propagate the length of the cell was taken as one-half the average time between received signals. In a few instances only one received pulse was present. It was then necessary to apply a small correction to the measured time interval. The correction time was taken as the difference between the transit time and the first time interval for the previous crystal.

The distance between transducers L was determined by multiplying the transit time in liquid ^{3}He by the known sound velocity in the liquid.[28] The measured transit time was 24.14 μsec at a pressure of 32.82 bar and at a temperature of 1.00 K. The sound velocity (407 m/sec) under these conditions was determined by graphically interpolating between the values tabulated by Vignos and Fairbank[28] for a 98% ^{3}He sample. The path length at 1 K was calculated to be 0.982 cm. The length of the cell at room temperature, measured with precision micrometers, was 0.9949 cm. The thermal contraction $\Delta L/L$ was therefore 0.013, in line with published[29] values of 0.0139 for nylon and 0.0155 for polystyrene. The possible systematic error in the absolute velocity due to the uncertainty in the length of the cell is estimated to be less than 0.5%.

G. Procedure

The vacuum space surrounding the cryostat was in common with the main Dewar vacuum. As a consequence several days were required to cool the system down to below 4 K. Cooling to near liquid-nitrogen temperature was accomplished by leaving the Dewar vacuum slightly soft and transferring liquid nitrogen into the nitrogen reservoir. This required about 36 h. During this time a 6-psi ^{4}He gas pressure was maintained in the ^{4}He-refrigerator pump-out tube (see Fig. 2) in order to prevent a plug from developing in the flow impedance. An overpressure of ^{4}He gas was also maintained in the main helium reservoir and in the thermal shorting tube. Liquid helium was then transferred into the helium reservoir. The apparatus was slowly cooled to the bath temperature by liquid reflux in the ^{4}He-refrigerator pump-out tube and in the shorting tube. The heat switch was in the closed position. After 24 h each of the platforms was at 4 K. The shorting tube was then evacuated, eliminating most of the thermal connection between the 1- and 0.3-K platforms. The ^{4}He and ^{3}He refrigerators were started. Within a half hour the platform temperature was below 0.5 K. The high-purity ^{3}He gas was now condensed into the freezing cell and into a 6-cm^3 pressure-generating bomb located in a second helium Dewar whose bath was pumped to below 1.2 K. The bomb was situated inside a brass can filled with helium exchange gas. When the condensation was complete the storage cylinder was closed off from the system and the helium transfer gas removed from the brass can. The working pressure was generated by slowly heating the bomb. With the pressure manually regulated at the desired level and the temperature electronically regulated at approximately 0.01 K above the corresponding freezing temperature, the pressure generator was separated from the system (valve No. 5 closed, Fig. 4). Because of the diffusion of ^{3}He through the quartz bourdon tube, the Texas Instruments pressure gauge also was now removed from the system, leaving only a temperature-regulated 100-cm^3 volume reservoir joined to the cell. From this point on to the conclusion of the experiment the gas manifold remained untouched. The main bulk of the data was obtained during a run which lasted for 42 days. During this period the sample-platform temperature was never raised above 1 K.

The 100-cm^3 room-temperature volume reservoir was large compared with the volume of the cell; thus the crystals could be grown under nearly-constant pressure conditions. The change in pressure upon freezing was less than 1%. The crystal-growing procedure consistently yielding the highest-quality samples began with the cell being regulated at a temperature approximately 0.15 K above the freezing temperature T_f. At this time the heat switch was in a fully closed portion and 4 μW of power were being dissipated in the capillary anchor heater (see Fig. 2). After temperature differences between the top and bottom of the cell had decayed, the temperature regulator was turned off resulting in the rapid decrease in the temperature of the bottom of the cell. The temperature continued to fall at a rate of ~0.020 K/min until a crystal nucleated. After the recovery of the solid from the supercooling of the liquid, the temperature of the cell bottom T_B decreased at a rate of ~0.0013 K/min until solid completely filled the cell. With no more latent heat to be carried away, the cell bottom temperature again decreased quickly and temperature gradients across the cell decayed. After the crystal had cooled to approximately 0.38 K, the x-ray photographs were taken and the sound-velocity measurements made. The crystal was then melted by dissipating a few microwatts of power in both the heater wrapped around the capillary and in the capillary anchor heater while the sample platform was raised up to T_f +0.15 K. After a sharp cooling spike registered on the cell thermometer, indicating that the capillary was free of solid, the capillary heater was turned off. In about 1 h, tempera-

ture gradients in the cell had decayed away. The system was now set for the whole process to be repeated.

The melting of several crystals was carried out much more carefully in order to accurately determine the melting temperature T_m and hence the molar volume[30] of the samples. Because the samples were not grown under strictly constant pressure the melting temperature differed slightly from the freezing temperature. Figure 5 is a strip-chart recorder tracing showing the temperature of the bottom of the cell as the crystal was slowly warmed to its melting point. The trace shows a considerable overshoot of the melting temperature which was determined by extrapolating the nearly linear warming curve in the two-phase region back to the warming curve of the solid. Although the melting temperature of a particular sample could be determined to within about 1 mK, it was only carefully measured for a few samples and differed between determinations by a few millidegrees. The melting temperature for all samples was taken to be 0.680 ± 0.003 K. This corresponds[30] to a molar volume of 24.45 ± 0.01 cm^3 and to a melting pressure of 32.82 ± 0.05 bar, in agreement with the pressure measured at the beginning of the experiment.

Attempts were made to grow crystals at much slower growing rates, with one sample being grown over a period of 12 h. These samples were all of extremely poor quality due to the lack of a single nucleation point. On the other hand, high-quality single crystals were consistently grown at the fastest growing rates presumably because sizeable temperature gradients in the cell forced nucleation to take place only at a single point.

Several attempts to improve the quality of strained or polycrystalline samples through annealing were made. In one sample complete recrystallization took place yielding an excellent crystal. However, in the four other attempts no meaningful improvements were made. One of these samples was held at $T_m - 0.01$ K for 44 h.

III. RESULTS AND DISCUSSION

A. Sound velocities

In the course of the present study 104 solid ^{3}He samples in the bcc phase were grown at a molar volume of 24.45 cm^3. The first ten samples were grown under various conditions in an attempt to find a "best" growing technique and on these crystals no velocity measurements were made. Of the remaining 94 samples, only 36 were high-quality single crystals with strong ultrasonic signals. The other samples for which no velocity data could be obtained roughly fell into three groups: those with poor crystal quality, i.e., severely strained or polycrystalline samples; those whose x-ray photographs showed only one diffraction spot or no diffraction spots at all; and those whose orientation was such that no ultrasonic signal could be detected.[16]

Several x-ray photographs showed only two (110)-type diffraction spots separated by 60° or 120°. For these samples it was not possible to determine uniquely the orientation from the Laue photographs alone. It was necessary to eliminate one of the two possible orientations, which are related by a 60° rotation about a ⟨111⟩ axis, by comparing the measured sound velocities with the expected sound velocities for the two orientations. A stereographic projection constructed from one of the Laue photographs in which only two (110)-type reflections were detectable is shown in Fig. 6. From the projection it was only possible to determine that the orientation was such that the direction of wave propagation (the axis of the cell), relative to the major axis of the cubic crystal, was either described by spherical-coordinate angles $\theta, \varphi = 43°, 45°$ (solid curves) or by $\theta, \varphi = 27°, 45°$ (dashed curves). The angles θ and φ are defined in the figure. However, the measured longitudinal velocity of 487 m/sec and the slow-transverse velocity of 166 m/sec were both very close to the values implied for $\theta, \varphi = 43°, 45°$ by measurements of the sound velocities in other directions in crystals with unambiguous orientation. For the second orientation, the expected longitudinal velocity was about 25 m/sec smaller, while the expected slow-transverse velocity was about 25 m/sec faster than the observed velocities. It was thus possible to assign a unique orientation to the crystal.

For seven of the data crystals both transverse and longitudinal velocities were measured. In

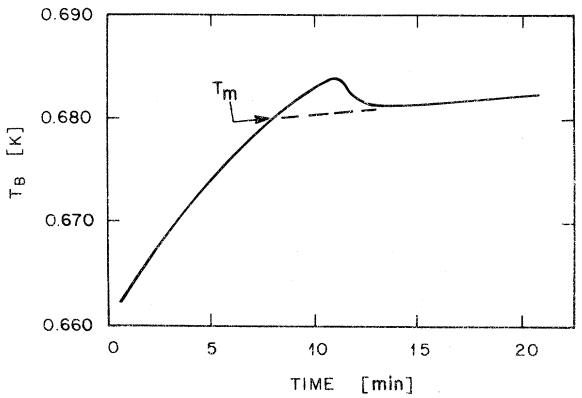

FIG. 5. Temperature measured at the bottom of the freezing cell as a ^{3}He crystal was warmed to its melting point versus time (arbitrary origin).

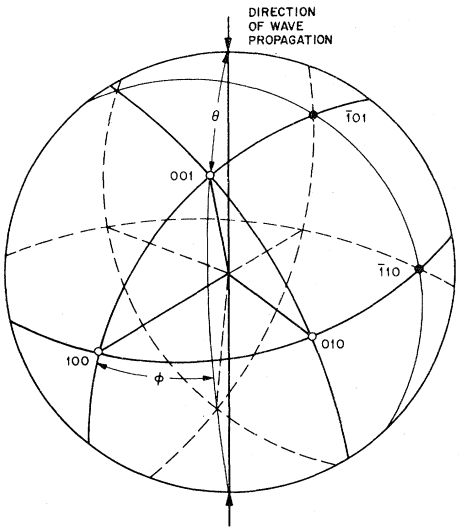

FIG. 6. Stereographic projection constructed from one of the Laue photographs in which only two (110)-type diffraction spots were detectable. One of the two possible orientation of the crystal is indicated by the solid curves; $\theta, \varphi = 43°, 45°$. The second possible orientation, related to the first by a 60° rotation about the [111] axis, is indicated by the dashed curves; $\theta, \varphi = 27°, 45°$. The measured sound velocities were consistent only with the first orientation.

these samples the two signals could easily be distinguished. At a low transducer driving voltage only the transverse signal was detected. At higher driving voltages the weaker longitudinal signal was made sizable, with echos still being observable long after the last detectable transverse signal.

There was thus a total of 43 data points: 26 longitudinal L, 16 fast-transverse T_1, and one slow-transverse T_2. Each of the data points consisted of the freezing temperature of the sample T_f, the longitudinal or transverse sound velocity measured at some temperature in the range 0.37–0.40 K, and the direction of sound propagation relative to the major axes of the crystal. In the temperature range 0.37–0.40 K, the sound velocities were constant within the precision of the measurements. This is consistent with the recent findings of Wanner *et al.*[14] The freezing temperature was recorded for each sample in order to verify that no leaks had developed in the system and thus that all samples were being grown at essentially the same density. With the exception of a few samples, the freezing temperatures of the data crystals differed by no more than 6 mK. Problems with the temperature controller on the reference volume (see Fig. 4) accounted for the few exceptions. For these samples a correction was applied to the measured velocity. The correction was made assuming that the velocity was a linear function of the molar volume. In the worst case the correction was 0.7%.

The velocity data are listed in Table I and the direction of wave propagation for each of the data points is plotted on a stereographic projection of $\frac{1}{48}$th of the reference sphere in Fig. 7(a). All directions in the crystal are by symmetry equivalent to a direction in this unit triangle. The open and closed circles in the figure correspond, respectively, to propagation directions in which longitudinal or transverse velocities were measured using AC-cut quartz sound transducers; the half-closed circles indicate those directions for which both longitudinal *and* transverse signals were observed in the same crystal; and the open squares correspond to directions in which longitudinal velocities were measured using X-cut quartz transducers.

It is interesting to note that the samples grown when the cell contained the shear transducers had more or less-random orientations. On the other hand, four of the seven crystals grown when compressional transducers were used grew with the ⟨100⟩ axis within 10° of the cell axis. It is not clear, however, if the growth of crystals with preferred orientation was at all related to the cut of the transducers.

B. Elastic constants

The elastic constants for this cubic structure were determined by simultaneously fitting all of the velocity data with the three velocity surfaces determined by the elastic constants. The fit was performed using the expressions[31,32] relating each of the three sound velocities (longitudinal, fast transverse, or slow transverse) for waves propagating in arbitrary direction to the three reduced elastic constants C_{11}/ρ, C_{12}/ρ, and C_{44}/ρ, where ρ is the density. The nonlinear least-squares program used was based on the maximum-neighborhood method developed by Marquardt.[33] There was no weighting of the data. The results, in units of 10^9 cm^2/sec^2, are

$$\begin{aligned} C_{11}/\rho &= 1.634 \pm 0.020\,, \\ C_{12}/\rho &= 1.356 \pm 0.033\,, \\ C_{44}/\rho &= 0.753 \pm 0.010\,, \\ (C_{11} - C_{12})/2\rho &= 0.139 \pm 0.022\,. \end{aligned} \tag{2}$$

The uncertainties quoted here are standard errors in the parameters. The assumption was made that the errors in the velocity data arising from errors in the crystal orientation were random. This assumption is not strictly valid; however, it should not significantly affect the results. The calculation of the standard errors takes into account cor-

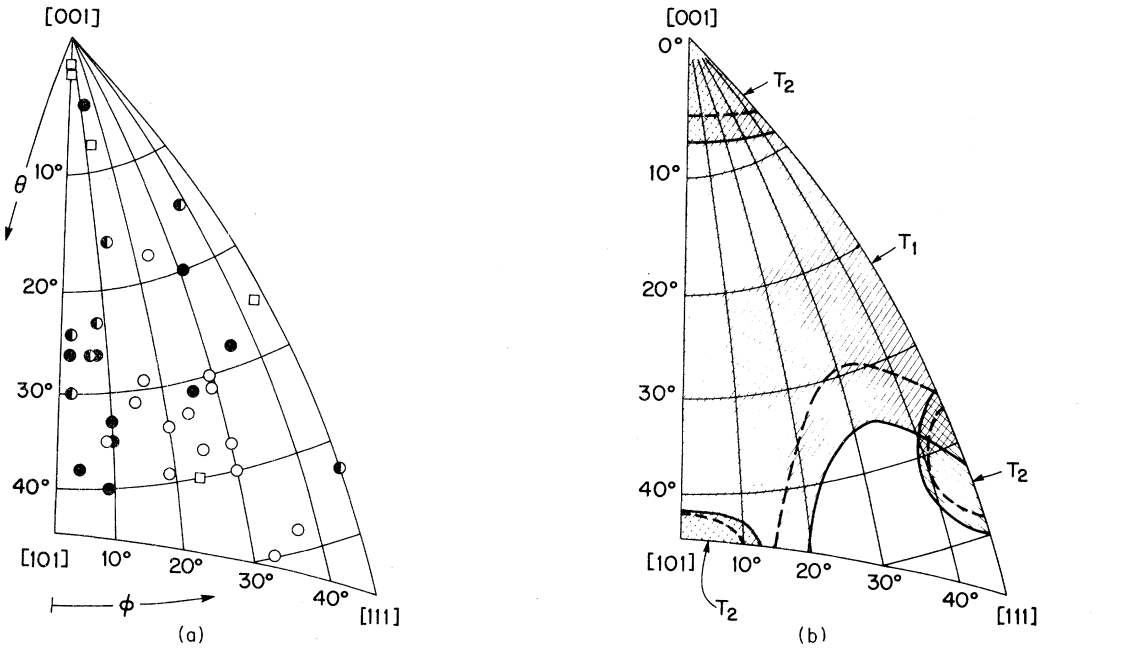

FIG. 7. Direction of wave propagation for each of the sound-velocity data points listed in Table I and (b) the regions allowed by the geometry of the cell for the detection of a fast-transverse T_1 or slow-transverse T_2 signal, plotted on stereographic projections of the unit triangle. The open and closed circles correspond, respectively, to propagation directions in which longitudinal or transverse velocities were measured using AC-cut quartz sound transducers; the half-closed circles indicate those directions for which both longitudinal *and* transverse signals were observed in the same crystal; and the open squares correspond to directions in which longitudinal velocities were measured using X-cut quartz transducers. In (b), the boundaries of the shaded areas correspond to a maximum deviation between the sound beam and the wave normal of 32°. The reduced regions that would be bounded by the dashed curves correspond to a deviation of 27°.

relations between the fitting parameters. The significant correlations between C_{11} and C_{12} and hence the uncertainties in these elastic constants would have been reduced had it been possible to obtain several measurements on the slow-transverse velocity surface, particularly near ⟨110⟩. Velocities on this surface are dominated by a difference between C_{11} and C_{12}, whereas on the longitudinal surface, where most of the data were obtained, it is a sum of the two constants which is important. The fast-transverse surface is most strongly influenced by C_{44}. Values of the sound velocities calculated using the constants given in Eq. (2) are listed in Table I in order to provide a direct comparison with the measured values. The relative difference is also tabulated. The measured longitudinal velocity for $\theta, \varphi = 50°, 33°$ differs from the calculated velocity by 2.4%, a value larger than any of the other differences given in the table. The ultrasonic signal for this sample showed one strong pulse which at first appeared to correspond to a velocity of 100 m/sec preceded by two much weaker signals corresponding to a longitudinal velocity of about 500 m/sec; however, the orientation of this sample was such that a transverse velocity of 100 m/sec would have been inconsistent with the remainder of the data. It appears now that the strong pulse was the third received longitudinal signal. Interference caused by the signal propagating through at least two crystals with very nearly the same orientation could explain the strange echo pattern. Consistent with this explanation, the x-ray-diffraction spots did show some structure, and the ultrasonic pulses did have rather poor rise times. It is reassuring to note the small relative difference associated with the only measurement in this study of a slow-transverse velocity in a crystal whose orientation was determined using x rays. We have thus a direct demonstration that measurements on the longitudinal and fast-transverse surfaces alone can be used to determine quite accurately the slow-transverse surface.

The sound velocities for the wave-propagation vector $\hat{k}$ (i.e., the normal to the wave front) lying in the (100) and (110) planes, calculated using the elastic constants given in Eq. (2), are plotted in Fig. 8(a). If no two velocities are equal it is necessary that the displacement vectors be mutually perpendicular.[34] It is not necessary, in general,

TABLE I. Sound velocities in bcc ^{3}He at a molar volume of 24.45 cm^3. The angles θ and φ are the spherical coordinates of the direction of sound propagation relative to the principal axes of the crystal. The calculated velocities are those determined by the three elastic constants [Eq. (2)] resulting from a least-squares fit of all of the data.

Mode	θ (deg)	φ (deg)	Measured velocity (m/sec)	Calculated velocity (m/sec)	Relative difference
Longitudinal L	2	1	407	405	0.005
	3	0	411	406	0.012
	8	12	413	413	0.000
	15	38	422	430	−0.019
	16	13	433	432	0.002
	18	23	438	438	0.000
	23	8	443	449	−0.014
	24	2	451	451	0.000
	25	43	462	457	0.011
	26	6	460	455	0.011
	29	17	468	462	0.013
	30	2	460	462	−0.004
	30	29	465	467	−0.004
	31	15	466	465	0.002
	31	29	461	469	−0.017
	33	24	464	471	−0.015
	34	20	471	471	0.000
	35	19	477	472	0.010
	37	25	468	477	−0.019
	37	30	480	479	0.002
	39	19	474	477	−0.006
	40	24	480	480	0.000
	40	30	474	483	−0.019
	43	45	487	490	−0.006
	48	37	502	492	0.020
	50	33	503	491	0.024
Transverse T_1	5	12	277	274	0.011
	15	38	269	267	0.007
	16	13	272	273	−0.004
	20	31	260	265	−0.019
	23	8	270	273	−0.011
	24	2	279	274	0.018
	26	2	273	274	−0.004
	26	6	270	274	−0.015
	26	8	276	273	0.011
	28	35	254	252	0.008
	30	2	275	274	0.004
	31	26	257	257	0.000
	33	10	270	271	−0.004
	35	10	275	271	0.015
	38	4	271	274	−0.011
	40	9	270	271	−0.004
Transverse T_2	43	45	166	167	−0.006

however, that the displacements be either parallel (pure longitudinal) or perpendicular (pure transverse) to the propagation vector. For $\hat{k}$ lying in a symmetry plane it is necessary that one of the mutually perpendicular displacements be perpendicular to the plane, that is, one wave must be purely transverse. The other two waves with displacement vectors lying in the symmetry plane, provided that $\hat{k}$ is not along a higher-symmetry direction, are quasilongitudinal and quasitrans-

verse. The deviation δ_L of the quasilongitudinal displacement vector from its wave normal[35] calculated from the elastic constants is indicated in Fig. 8(b). The arrows in the figure indicate the sense of positive deviation. The maximum deviation is seen to be about 12°.

It is well known in the field of ultrasonics that the energy flux vector, the ray, may deviate substantially from the wave normal in anisotropic crystals. However, the significance of this effect in ^{3}He which is highly anisotropic $[2C_{44}/(C_{11}-C_{12})=5.4]$ had been overlooked until Wanner[16] pointed out that the deviations in bcc ^{3}He may be as large as 60°. The rays associated with a wave propagation vector lying in one of the cubic symmetry planes also lie in the plane. Thus it is possible to plot in Fig. 8(c) the ray deviations Δ calculated[35] from the elastic constants. Again the arrows in the figure indicate the sense of positive deviation. With the geometry of the present sound cell, rays which have $|\Delta| \gtrsim 32°$ will not strike the opposite transducer before all of the beam is reflected by the curved walls of the cell. This would result in the beam losing phase coherence over its cross section and becoming undetectable. It is evident

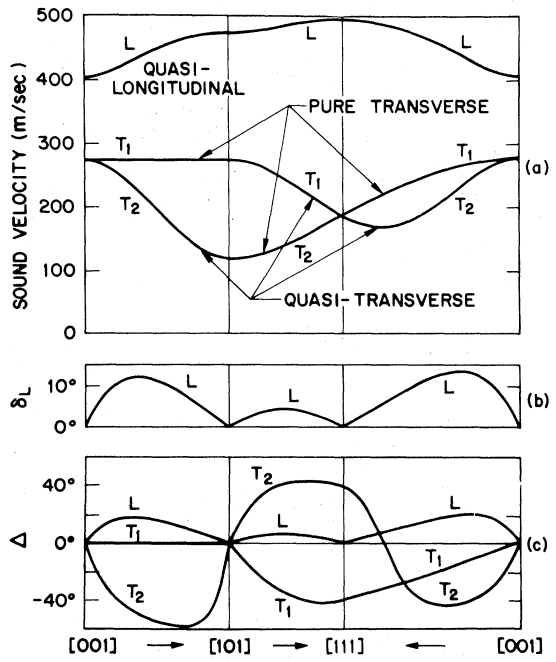

FIG. 8. (a) Longitudinal and transverse sound velocities; (b) the deviation of the quasilongitudinal displacement vector from the wave normal; and (c) the deviations of the sound rays from the wave normal, plotted for wave propagation vectors lying in the cubic symmetry planes. The curves were calculated using the elastic constants of bcc ^{3}He given in Eq. (2). The arrows indicate the sense of positive deviations.

from the figure that $|\Delta_L|$ is always less than 32° and thus that a longitudinal signal should be detectable for all $\hat{k}$. This is not true for either the fast or the slow transverse waves.

The deviations for arbitrary $\hat{k}$ have also been computed. The regions in the unit triangle for which T_1 or T_2 signals should be detectable (that is, regions with $|\Delta_{T_1}|<32°$ or $|\Delta_{T_2}|<32°$) are indicated by the shaded areas in Fig. 7(b). A comparison with Fig. 7(a) shows that all of the velocities were measured in allowed regions. In fact no T_1 or T_2 velocity was measured which had a calculated deviation of greater than 27°. The reduced regions corresponding to deviations of less than 27° are bounded by the dashed curves in the figure. It is obvious that with the present cell design crystals grown with random orientations have a small probability of being oriented such that velocities on the slow-transverse surface can be measured. Of course by going to pancake-shaped cells the chances of observing this mode are greatly increased; however, it is then difficult to probe the crystal with x rays. In one sample a T_1 velocity of 272 m/sec and a T_2 velocity of 116 m/sec were measured. Unfortunately the x-ray photographs showed no discernable diffraction spots. This does not necessarily mean that the sample was not a single crystal. If, for example, the crystal were oriented such that the ⟨100⟩ direction was paralled to the x-ray beam, then the (200)-type reflections would coincide with the beam and the (110)-type reflections would come off at an angle much larger than the open angle of the windows in the tail of the Dewar. Since no other types of reflection are intense enough to be detected, the film would show no diffraction spots at all. Assuming then that a single crystal filled the cell, its orientation could only be such that the propagation direction was in one of the small regions allowed for detection of a T_2 velocity. From the magnitude of the T_1 and T_2 velocities it is obvious that the measurements were made in the region near ⟨110⟩. It should be noted that having the ⟨110⟩ direction parallel to the axis of the cell is not inconsistent with having the ⟨100⟩ direction parallel to the x-ray beam. The measured slow velocity is in excellent agreement with the ⟨110⟩ velocity determined from the elastic constants, namely, 118 ± 10 m/sec.

It is evident that simply being able to detect or even not being able to detect an ultrasonic signal can, in some cases, give useful information concerning the orientation of a helium crystal. As another example, Wanner has noted that a few of the sound velocities presented by Greywall and Munarin[36] and by Greywall[13] were measured in directions that were forbidden by the geometry of

their cell. These measurements were made in x-ray-oriented crystals of bcc ^{3}He at a molar volume of 21.66 cm^3. This discrepancy prompted a re-evaluation of the data. Keeping only those crystals whose Laue photographs implied high-quality crystals *and* whose oscilloscope-trace photographs indicated strong clean ultrasonic signals resulted in the elimination of several data points. The points that were eliminated were generally those whose velocities deviated most from the least-squares values. The more selective screening of the data left no crystals with orientations in the forbidden regions. A least-squares fitting of the reduced set of 37 data points at 21.66 cm^3/mole yielded, in units of 10^9 cm^2/sec^2,

$$\begin{aligned} &C_{11}/\rho = 2.727 \pm 0.033\,, \\ &C_{12}/\rho = 2.477 \pm 0.058\,, \\ &C_{44}/\rho = 1.422 \pm 0.021 \\ &[(C_{11} - C_{12})/2\rho = 0.125 \pm 0.039]\,. \end{aligned} \tag{3}$$

The constants correspond to sound velocities measured at ~1.2 K. Comparing these results with those quoted in the original paper[13] shows that the only significant change (4%) is in C_{12}/ρ. However, as an important consequence $(C_{11} - C_{12})/2\rho$ is considerably larger which implies that the calculated Debye temperature will be much closer to $\Theta_D^{\max}$. It should also be noted that even though the constants given above provide a better fit of the data the uncertainties are not reduced. The present larger more realistic uncertainties include the effect of correlations between parameters, whereas the previously published results do not.

The elastic constants determined by the present measurements at 24.45 cm^3/mole and the re-evaluated constants at 21.66 cm^3/mole are plotted in Fig. 9 as closed and open circles respectively. In addition to the nonsystematic errors which account for the uncertainties quoted for each of the constants in Eqs. (2) and (3), estimates of possible systematic errors are also included. These errors arise from the $\frac{1}{2}$% uncertainty in the ultrasonic path length and from uncertainties in the determination of the molar volume, ± 0.01 cm^3/mole at 24.45 cm^3/mole, and ± 0.05 cm^3/mole at 21.66 cm^3/mole. At 24.45 cm^3/mole the total uncertainty in the three elastic constants is less than the size of the symbol in the figure. In order to facilitate comparison with elastic constants determined by others at intermediate molar volumes, dashed lines have been drawn in the figure joining the data at the two molar volumes assuming that the mode Grüneisen parameter[37]

$$\gamma_{ij} \equiv -\frac{1}{2}\frac{d\ln C_{ij}}{d\ln V} - \frac{1}{6} \tag{4}$$

is independent of molar volume V. Measurements of the shear velocity in bcc ^{3}He have been made by Lipschultz and Lee[12] and by Lipschultz[38] at several molar volumes between 23.80 and 24.40 cm^3 near the respective melting temperatures. The data were taken in crystals of unknown orientation; however, Wanner[16] has pointed out that the velocities measured must correspond, due to the geometry of the cell, to sound propagating in directions close to the (100) plane. In the allowed region for detection of the T_1 shear waves, the velocity is nearly constant. The measured velocities thus yield C_{44} to within about 5%. At two densities these results for C_{44} are shown in the figure as open squares. The agreement with C_{44} determined by the present measurements is excellent. The open squares corresponding to the other two elastic constants, C_{11} and C_{12} were not determined by measurements of the sound velocity alone. These constants were inferred by Wanner using in addition to C_{44}, measurements of the compressibility and of the Debye temperature Θ_D, quantities which are simply related to the elastic constants. A problem arises in this analysis, however, since it is not clear from the specific-heat measurements what the value of Θ_D actually is. Wanner was forced to assume that Θ_D was within 10% equal

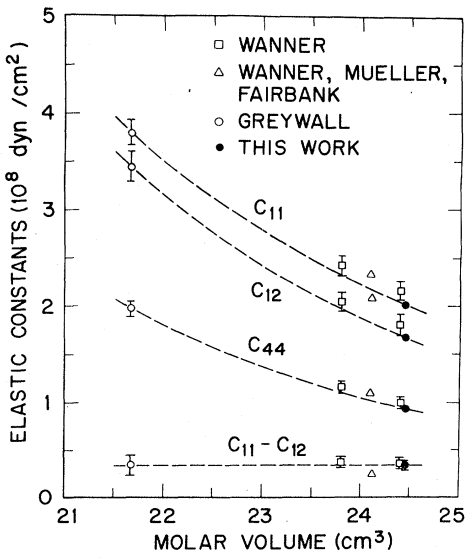

FIG. 9. Elastic constants of bcc ^{3}He versus molar volume. The elastic constants [Eq. (2)] determined by the sound velocities measured in the present study and the elastic constants [Eq. (3)] resulting from a reanalysis of the sound velocities measured by Greywall (Ref. 13) are compared with those inferred by Wanner (Ref. 16) and those extracted from sound-velocity measurements in unoriented crystals by Wanner *et al.* (Ref. 14). The dashed curves were drawn only to aid in the comparison.

to $\Theta_D^{\max}$. It is now apparent from the fine agreement between these constants and the directly determined constants of the present work that this assumption is justified. In the figure we also show as open triangles the elastic constants recently determined from sound-velocity measurements by Wanner, Mueller, and Fairbank[14] at 24.1 cm^3/mole and near the melting temperature. These velocity measurements were made in a very flat cell which permitted the velocity of sound waves propagating in any direction to be measured. However, no direct determinations of the orientations of the crystals were made. It was necessary to calculate the elastic constants under the assumption that the fastest and slowest longitudinal and transverse velocities measured in 20 samples corresponded to the actual velocities in the appropriate symmetry directions. Of course meaningful upper and lower error bars cannot be assigned to each of these constants. It is therefore difficult to compare these constants with those determined in the present work. Instead it is simpler to compare directly their observed limiting velocities with the corresponding velocities calculated from the elastic constants interpolated between the constants at 24.45 and 21.66 cm^3/mole using Eq. (4). Although we would have expected perhaps to find faster fastest velocities and slower slowest velocities we instead find a fastest transverse velocity which is about 4% *less* than their value, a fastest longitudinal velocity about 5% *less* than their value, and a slowest transverse velocity which is about 14% *greater* than their corresponding velocity. These are differences which are greater than the expected combined uncertainties. The discrepancies of 4 and 5% might tend to suggest that the systematic errors in one or both of the experiments may have been underestimated, however this would not explain the difference in the two determinations of the slow transverse velocity in the ⟨110⟩ direction.

It is to be noted that we have been comparing elastic constants[14,16] which correspond to the crystal being near the melting temperature with elastic constants which were determined at lower temperatures. The elastic constants do have a temperature dependence; however, this dependence is small. The precise measurements of the change in the sound velocity with temperature by Wanner *et al.*[14] at 24.1 cm^3/mole indicate that the elastic constants change by no more than a few tenths of a percent between 0.123 and 0.800 K. At 21.66 cm^3/mole it is expected[15] that the temperature dependence of the elastic constants below 1.2 K, the temperature at which the sound velocities were measured, is also small. Thus all of the constants shown in the figure can be treated to an approximation much smaller than their uncertainty, as 0-K constants.

C. Compressibility

A check on the estimates of the total uncertainties in the measured elastic constants can be made by comparing the volume compressibility β_v determined by the elastic constants with β_v resulting from thermodynamic measurements. In the cubic system the compressibility is related to the elastic constants via the simple equation[39]

$$\beta_v = 3/(C_{11} + 2C_{12}) . \tag{5}$$

By substituting from Eq. (2) and (3) the values of the appropriate adiabatic constants we find at 24.45 cm^3/mole,

$$\beta_v^s(0.4\ \text{K}) = (5.594 \pm 0.067) \times 10^{-3}\ \text{bar}^{-1} \tag{6}$$

and at 21.66 cm^3/mole,

$$\beta_v^s(1.2\ \text{K}) = (2.804 \pm 0.035) \times 10^{-3}\ \text{bar}^{-1} . \tag{7}$$

The superscript s denotes that the compressibility has been determined under adiabatic conditions. We would like to compare these values of the adiabatic compressibility with the *isothermal* compressibility β_v^T along the melting curve derived from PVT data by Grilly.[30] It is thus necessary to relate $\beta_v^s(T)$ to $\beta_v^T(T_m)$. The recent measurements of the temperature dependence of the sound velocity by Wanner *et al.*[14] at 24.1 cm^3/mole indicate that β_v^s at 24.45 cm^3/mole will decrease by less than 0.1% as the temperature is warmed up to the melting temperature. At T_m the difference between the adiabatic and isothermal compressibility can be calculated by applying the thermodynamic relation

$$\beta_v^T - \beta_v^s = \alpha^2 VT/C_p \approx \alpha^2 VT/C_v . \tag{8}$$

Using the values of the thermal-expansion coefficient α given by Grilly[30] and of the specific heat C_v given by Castles[40] this difference is found to be of the order of a few tenths of 1% of β_v^s. Thus to a good approximation we have at 24.45 cm^3/mole, $\beta_v^T(T_m) \approx \beta_v^s(0.4\ \text{K})$. At 21.66 cm^3/mole we first calculate $\beta_v^T(1.2\ \text{K})$ using Eq. (8) with C_v taken from the work of Castles and α from the work of Straty and Adams.[41] The difference $\beta_v^T - \beta_v^s$ amounts to about 0.6% of β_v^s. The change in β_v^T as the melting temperature is approached is estimated from the results of Straty and Adams to be about 3%. The two values of the isothermal compressibility along the melting curve are plotted in Fig. 10, the value at 24.45 cm^3/mole as a closed circle, the value at 21.66 cm^3/mole as an open circle. The error bars include, in addition to the statistical uncertainty given in Eqs. (6) and (7), estimates of possible,

systematic errors, but do not include any estimates of errors introduced in the convertion of $\beta_v^S(T)$ to $\beta_v^T(T_m)$. The results are seen to be consistent, within the experimental uncertainties, with the thermodynamic measurements. The compressibility determined by Wanner *et al.*[14] is indicated in the figure as an open triangle and is about 9% smaller than the corresponding thermodynamic value. However, as mentioned earlier, due to the indirect method in which the orientations of their samples were determined, it is not possible to attach meaningful error bars to their elastic constants or thus to their compressibility. It might be noted though that a systematic error of ~4½% in their sound-velocity measurements could explain the 9% difference between the compressibility determined by their elastic constants and the thermodynamic value as well as account for the discrepancy between their fastest observed longitudinal and transverse velocities and the corresponding velocities determined in the present work.

D. Debye temperature

According to the Debye theory, the Debye temperature can be calculated from the sound velocities using the relation

$$\Theta_D = (h/k_B)(3N/4\pi)^{1/3} v_D , \tag{9}$$

where k_B is Boltzmann's constant, N is the number of atoms per unit volume, and the Debye velocity v_D is defined by

$$v_D = \left((12\pi)^{-1} \int \sum_i \frac{1}{v_i^3} \, d\Omega \right)^{-1/3} .$$

In this theory Θ_D is a constant which can be used to predict C_v at all temperatures. In a real system, however, the sound velocities and Θ_D calculated using Eq. (9) are temperature dependent due to anharmonicity. The Debye temperature determined from calorimetric data must also reflect this temperature dependence; here though a more significant contribution to the temperature dependence arises from dispersion in the phonon spectrum. The long-wavelength phonons probed by sound-velocity measurements are the dominant phonons contributing to the specific heat only for $T \approx 0$ K. Thus it is only in this limit that the elastic Debye temperature $\Theta_D^e(T)$ and the calorimetric Debye temperature $\Theta_D^c(T)$ should be identical; that is, $\Theta_D^e(0\text{ K}) \equiv \Theta_D \equiv \Theta_D^c(0\text{ K})$.

In general then, one may need to go to quite low temperatures with either method in order to obtain an accurate determination of Θ_D. A difficulty often arises in the thermal measurements since in addition to the phonons other excitations of known or unknown origin may contribute appreciably to the total specific heat and prevent the extraction of Θ_D from the data. One must then rely on Θ_D determined by the zero-temperature elastic constants. This is precisely the situation for bcc ^{3}He.

As noted earlier, the temperature dependence of the sound velocities has been recently measured in ^{3}He crystals of unknown orientation between the melting temperature and 0.123 K.[14] The results show that at large molar volumes, the temperature dependence is weak. Between 0.4 and 0.123 K the sound velocities change by less than 0.04%. The present measurements of the sound velocities at 0.4 K in crystals of known orientation can thus be used to accurately determine Θ_D.

The integral in Eq. (9) was evaluated numerically using the sound velocities determined by the elastic constants given in Eq. (2). The calculation yielded $\Theta_D = 18.53 \pm 0.66$ K. The uncertainty in Θ_D was found by recalculating Θ_D with the three elastic constants adjusted within the limits stated in Eq. (2) to give the largest and smallest allowed value. The uncertainty in Θ_D most closely reflects the uncertainty in $\frac{1}{2}(C_{11} - C_{12})$, the modulus which corresponds to the slow transverse velocity in the ⟨110⟩ direction. The additional uncertainty in Θ_D due to possible systematic errors has been included in Fig. 11 where a comparison is made with the recent specific-heat results of Castles and Adams[6] and Castles.[40] The present results are

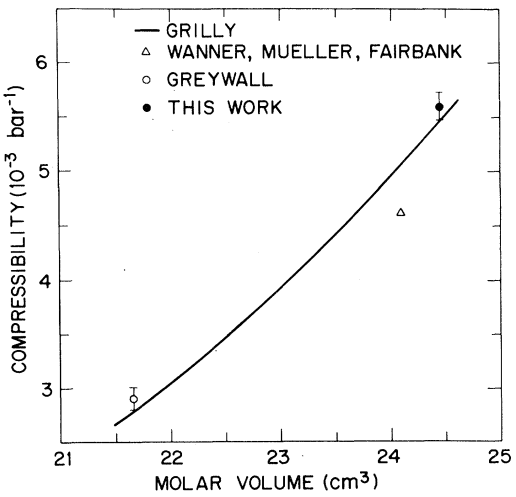

FIG. 10. Isothermal compressibility of bcc ^{3}He along the melting curve versus molar volume. The solid curve was drawn using the thermodynamic values tabulated by Grilly (Ref. 30). The symbols correspond to values calculated using the elastic constants given by Wanner *et al.* (Ref. 14), the elastic constants resulting from a reanalysis of the sound velocity measurements of Greywall (Ref. 13), and the elastic constants determined in this work.

seen to be in excellent agreement with the lower set of data points which correspond to $\Theta_D^{\max}$. The measured specific heat in the region of the anomaly can be described well by $C_v = AT + BT^3$. The upper set of data points labeled Θ_D' corresponds to the Debye temperature calculated assuming that the term in T^3 represents all of the lattice specific heat. If this assumption is valid then, of course, we should have expected the present determination of Θ_D to lie on the upper curve. At 21.66 cm^3/mole the elastic constants given in Eq. (3) imply $\Theta_D = 22.6^{+1.4}_{-1.7}$ K. Again, the value plotted in the figure also includes an estimate of possible systematic errors. It should be noted that this value is considerably different from the value 19^{+2}_{-3} K reported in an earlier publication.[13] The new value results from a reanalysis of the old data which has already been discussed. The error bars do not include $\Theta_D^{\max}$; however, $\Theta_D = \Theta_D^{\max}$ cannot be considered as inconsistent with the data. It should also be remembered that the sound velocities at this molar volume were measured near 1.2 K. We might then expect the calculated Debye temperature to differ from the true zero-temperature value by a few percent.[15] The open triangle in the figure is actually an upper limit to Θ_D determined by Wanner *et al.*[14] from sound-velocity measurements in unoriented crystals. This value is consistent with the present results and may not be inconsistent with $\Theta_D = \Theta_D^{\max}$.

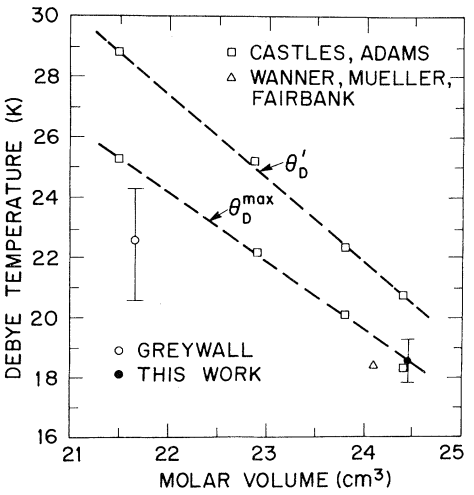

FIG. 11. Comparison of Θ_D determined by the elastic constants with values determined from the calorimetric data of Castles and Adams (Refs. 6 and 40) assuming that $\Theta_D = \Theta_D^{\max}$, lower curve, or assuming that the anomalous contribution to the specific heat is not due to the lattice and has a linear temperature dependence, upper curve labeled Θ_D'. The elastic Θ_D at 21.66 cm^3/mole was determined using the elastic constants resulting for a reanalysis of the sound-velocity data of Greywall (Ref. 13). The open triangle corresponds to the work of Wanner *et al.* (Ref. 14), the closed circle to the present work. The dashed lines were drawn only to aid in the comparison.

We find that, contrary to an earlier statement,[13] Θ_D may be equal to $\Theta_D^{\max}$ and thus that there is no experimental evidence to suggest that any of the excess specific heat must be due to an anomalous phonon dispersion. We also find that $\Theta_D = \Theta_D'$ is not allowed by the elastic measurements. It appears, as a consequence, that the excess specific heat must have other than a linear temperature dependence.

IV. SUMMARY

The longitudinal and transverse sound velocities were measured in single crystals of bcc ^{3}He at 24.45 cm^3/mole and at 0.4 K. A pulse-echo technique was used to measure the sound velocities. The crystal quality and orientation were determined from analyses of transmission Laue x-ray photographs. The complete set of elastic constants was determined by a least-squares fitting of the data which consisted mainly of sound-velocity measurements on the longitudinal and fast-transverse (T_1) surfaces. Two direct measurements on the slow-transverse (T_2) velocity surface are in excellent agreement with the appropriate velocities calculated using these elastic constants. Previously published[13] sound-velocity data at 21.66 cm^3/mole were reanalyzed. The new set of constants imply that $C_{11} - C_{12}$ and hence Θ_D are greater than had been reported. The compressibilities determined by the elastic constants at both 24.45 and 21.66 cm^3/mole are in excellent agreement with the corresponding compressibilities resulting from thermodynamic measurements. The Debye temperatures calculated using the elastic constants at both densities are not inconsistent with $\Theta_D = \Theta_D^{\max}$.

The experimental evidence consisting of (i) the measurements[6] of the specific heat down to 65 mK, (ii) the precise measurements[14] of the temperature dependence of the sound velocities down to 123 mK, and (iii) the present measurements of the sound velocities in crystals of known orientation indicate that certainly not all and possibly not any of the anomalous specific heat should be attributed to an anomalous phonon dispersion.

ACKNOWLEDGMENTS

We would like to thank W. O. Sprenger for purifying the ^{3}He sample and for calibrating the main thermometer at low temperatures, B. Golding for the loan of the ultrasonic electronics and for several helpful discussions, and G. Ahlers and N. R. Werthamer for reading and commenting on a manuscript of this paper.

[1]S. B. Trickey, W. P. Kirk, and E. D. Adams, Rev. Mod. Phys. 44, 668 (1972).
[2]H. H. Sample and C. H. Swenson, Phys. Rev. 158, 188 (1968).
[3]R. C. Pandorf and D. O. Edwards, Phys. Rev. 169, 222 (1968).
[4]P. N. Henriksen, M. F. Panczyk, S. B. Trickey, and E. D. Adams, Phys. Rev. Lett. 23, 518 (1969).
[5]W. C. Thomlinson, Phys. Rev. Lett. 23, 1330 (1969).
[6]S. H. Castles and E. D. Adams, Phys. Rev. Lett. 30, 1125 (1973).
[7]E. S. R. Gopal, *Specific Heats at Low Temperatures* (Plenum, New York, 1966).
[8]G. Ahlers, Phys. Lett. 22, 404 (1966).
[9]G. Ahlers, Phys. Rev. A 2, 1505 (1970).
[10]W. R. Gardner, J. K. Hoffer, and N. E. Phillips, Phys. Rev. A 7, 1029 (1973).
[11]H. Horner, J. Low Temp. Phys. 8, 511 (1972).
[12]F. P. Lipschultz and D. M. Lee, in *Proceedings of the Tenth International Conference on Low Temperature Physics* (VINITI, Moscow, 1967), Vol. 1, p. 309.
[13]D. S. Greywall, Phys. Rev. A 3, 2106 (1971).
[14]R. Wanner, K. H. Mueller, Jr., and H. A. Fairbank, J. Low Temp. Phys. 13, 153 (1973).
[15]D. S. Greywall, Phys. Lett. A 35, 67 (1971).
[16]R. Wanner, Phys. Rev. A 3, 448 (1971).
[17]1266, Emerson and Cummings, Inc., Canton, Mass.
[18]2850 FT, Emerson and Cummings, Inc., Canton, Mass.
[19]CryoCal, Inc., Riviera Beach, Fla.
[20]Driver-Harris Co., Harrison, N. J.
[21]L. E. DeLong, O. G. Symko, and J. C. Wheatley, Rev. Sci. Instrum. 42, 147 (1971).
[22]Uniform Tubes, Inc., Collegeville, Pa.
[23]R. H. Sherman, S. G. Sydoriak, and T. R. Roberts, J. Res. Nat'l. Bur. Stand. (U.S.) A 68, No. 6 (1964).
[24]T. R. Roberts and S. G. Sydoriak, Phys. Rev. 102, 304 (1956).
[25]G. Ahlers, Phys. Rev. 171, 275 (1968).
[26]R. H. Sherman, in Ref. 12, Vol. 1, p. 188.
[27]Gollob Analytical Service Corporation, Berkeley Heights, N. J.
[28]J. H. Vignos and H. A. Fairbank, Phys. Rev. 147, 185 (1966).
[29]G. K. White, *Experimental Techniques in Low-Temperature Physics* (Clarendon, Oxford, England, 1968), Table F, p. 377.
[30]E. R. Grilly, J. Low Temp. Phys. 4, 615 (1971).
[31]R. F. S. Hearmon, *An Introduction to Applied Anisotropic Elasticity* (Oxford U.P., Oxford, England, 1961).
[32]D. S. Greywall, Ph.D. thesis (Indiana University, 1970) (unpublished).
[33]D. W. Marquardt, J. Soc. Ind. Appl. Math. 11, 431 (1963); IBM report (unpublished).
[34]F. J. Fedorov, *Theory of Elastic Waves in Crystals* (Plenum, New York, 1968).
[35]G. F. Miller and M. J. P. Musgrave, Proc. Roy. Soc. Lond. 236, 352 (1956); M. J. P. Musgrave, Rept. Prog. Phys. 22, 74 (1959).
[36]D. S. Greywall and J. A. Munarin, Phys. Rev. Lett. 24, 1282 (1970); 25, 261(E) (1970).
[37]J. A. Reissland, *The Physics of Phonons* (Wiley, New York, 1973).
[38]F. P. Lipschultz, Ph.D. thesis (Cornell University, 1966) (unpublished).
[39]J. F. Nye, *Physical Properties of Crystals* (Clarendon, Oxford, England, 1957).
[40]S. H. Castles, Ph.D. thesis (University of Florida, 1973) (unpublished).
[41]G. C. Straty and E. D. Adams, Phys. Rev. 169, 232 (1968).